Composite Structures 109 (2014) 1–7

Contents lists available at ScienceDirect

Composite Structures

journal homepage: www.elsevier.com/locate/compstruct

Impact evaluation in carbon fiber reinforced plastic (CFRP) laminates using eddy current pulsed thermography

Yunze He [a,b,*], Guiyun Tian [b,c], Mengchun Pan [a,b], Dixiang Chen [a]

[a] College of Mechatronics Engineering and Automation, National University of Defense Technology, Changsha 410073, PR China
[b] School of Electrical and Electronic Engineering, Newcastle University, Newcastle Upon Tyne NE1 7RU, United Kingdom
[c] School of Automation Engineering, University of Electronic Science and Technology of China, Chengdu 610054, PR China

ARTICLE INFO

Article history:
Available online 4 November 2013

Keywords:
A. Carbon fibers
B. Impact behavior
D. Non-destructive testing
D. Eddy current pulsed thermography

ABSTRACT

With the growing interest to use engineering composite structures, much attention is devoted to the development of non-destructive testing (NDT) techniques for impact evaluation. Eddy current pulsed thermography (ECPT) is an emerging NDT technique, which is firstly investigated for crack evaluation in carbon fiber reinforced plastic (CFRP) in 2011 and the preliminary results have shown the significant potential. However, the research is limited by the experimental conditions. In this work, the detection mechanism for carbon fiber structure and impact are analyzed through theoretic analysis and validated by experimental studies under reflection and transmission modes. Laminates impacted with different energies from 4 J to 12 J are characterised. The qualitative and quantitative conclusions for impact behavior understanding are outlined, which is helpful to develop the reliable instruments for quality control and in-service inspection of CFRP.

1. Introduction

In recent decades, there has been an increasing interest in the use of carbon fiber reinforced plastic (CFRP), in the aerospace, renewable energy and other industries, due to low weight and relatively good mechanical properties compared with traditional metals. However, Carbon fiber composite materials have relatively poor properties in the direction transverse to their reinforcing fibers, with notably low resistance to impact. Impact events are inevitable during the lifetime of a composite structure, occurring during both service and maintenance in the form of collisions with stones or tools. Such events can cause extensive internal delamination. This damage, while often difficult or even impossible to detect at the surface of the material, severely degrades the loadbearing capacity of the structure [1].

To achieve these problems, NDT techniques based on acoustic, like ultrasonic testing [2], acoustic emission [3,4] are widely used. More recently, fiber Bragg grating (FBG) sensors are shown to have sufficiently high sensitivity for sensing acoustic waves [1,5,6]. In addition, more and more NDT methods, such as eddy current [7], microwave [8], speckle shearing interferometry [9], and infrared (IR) thermography [10] are investigated. Eddy current thermography is an emerging NDT technique, which combines the advantages of conventional eddy current testing and thermal wave testing. It has greater inspection speed and depth, higher resolution than eddy current. Unlike flash thermography, eddy current thermography does not rely on the surface conditions of material under test. Comparing with ultrasound, it does not require the couplant. With respect to excitation methods, eddy current thermography can be classified into these groups: eddy current pulsed thermography (ECPT) [11], eddy current lock-in thermography [12] and eddy current pulsed phase thermography [13,14]. Eddy current pulsed thermography combines the advantages of pulsed eddy current (transient analysis and eddy current interpretation [15]) and merits of thermography (fast and high resolution), which has been widely used for damage detection in metallic alloy [16,17]. In 2011, it is firstly investigated for crack evaluation in CFRP [18] and the preliminary results show the significant potential. However, the research of eddy current pulsed thermography for CFRP inspection is limited by the experimental conditions as follows: (i) The previous work is conducted under reflection mode where excitation and data acquisition are carried out on the same side. The transmission mode, where the specimen is stimulated from one side whilst data is recorded on the opposite side, has not been studied. (ii) The previous work is focused on the artificial crack. The real damages like impact have not been studied and the qualitative and quantitative conclusions for impact evaluation are blank.

In this work, the inspection methods using eddy current pulsed thermography for real impact are investigated and compared

* Corresponding author at: College of Mechatronics Engineering and Automation, National University of Defense Technology, Changsha 410073, PR China. Tel.: +86 13467698133; fax: +86 731 84574994.
E-mail address: hejicker@163.com (Y. He).

0263-8223/$ - see front matter © 2013 Elsevier Ltd. All rights reserved.
http://dx.doi.org/10.1016/j.compstruct.2013.10.049

under reflection and transmission modes, and some qualitative and quantitative conclusions are outlined. The rest of the paper is organised as follows. Firstly, the defect characterization methods are analyzed through theoretic analysis in Section 2. Then, ECPT experimental set-up and CFRP impacted samples are introduced in Section 3, which is followed by experimental studies and discussion in Section 4. Finally, conclusions and future work are outlined in Section 5.

2. Methodology

Eddy current pulsed thermography is a measurement technique, which induces eddy current in conductive material and detecting reflected thermal waves from boundaries of interfaces [11,16]. Fig. 1 shows the basic diagram. There are two configurations: reflection mode where excitation and data acquisition are carried out on the same side and transmission mode where the specimen is stimulated from one side whilst data is recorded on the opposite side [19].

According to different skin effect by eddy current induction, eddy current pulsed thermography involves two heating modes: (i) Near-surface heating. In this case, the skin depth is much small and can be neglected [20]. For example, ferromagnetic metals with high permeability have a much smaller skin depth (about 0.04 mm at 100 kHz). Thus, surface defect characterization is based on the eddy current interruption [21] while inner defect characterization relies on the heat diffusion [17]; (ii) Volumetric heating. In this case, skin depth is much great. For example, the skin depth in CFRP with small conductivity (about 50 mm at 100 kHz) is significantly larger than the thickness of most real components [22].

Due to the small conductivity of CFRP and the great skin depth, the heating mode in CFRP is volumetric heating. If there is a surface defect like crack or wall thinning [23,24], it leads to distortion on eddy current distribution, as depicted in Fig. 1. The introduction of a slot in the EC path results in a diversion of the EC below the defect, causing an increase in EC density and resultant hot spots [21]. Thus, the defect area will show the high temperature (hot spot) under reflection mode. In addition, the heat will transfer to rear side (D) as the heat diffuse. Therefore, the surface defect also shows the hot spot at rear side under transmission mode. The conductivity of CFRP is inhomogeneous because of the carbon fiber structure and multi-layer structure. Some information at surface and rear surface (such as carbon fiber structure, and surface impact spot) can be observed in the heating phase, because they affect the eddy current distribution and then heating distribution. However, the inner information (the temperature difference by delamination) can be observed in the cool phase, because they mainly affect the heat diffusion. The specific mechanisms are discussed in detail as follows.

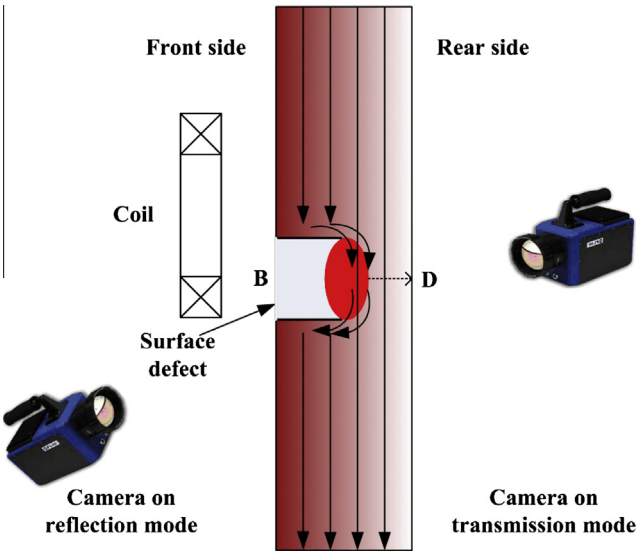

Fig. 1. Two detection modes for surface defect in CFRP.

2.1. Carbon fiber and polymer matrix

The commonly used precursor to manufacture carbon fibers is rayon. The lower modulus material has a fiber electrical conductivity of 40,000 S/m and high modulus is 190,000 S/m [25]. Normally, the matrix material is nonconductor. Therefore, carbon fiber based materials show a low electrical conductivity. In CFRP inspection using eddy current pulsed thermography, the induced eddy currents in the carbon fibers can heat the fibers directly. While, there is no induced EC heating in the polymer matrix and their heat is from surrounding carbon fibers. Therefore, the carbon fiber will show the higher temperature than polymer matrix in the heat phase under both reflection transmission modes.

2.2. Impact

It has been proven that electrical resistance increases when the impact energy increases using electrical resistance-based tomography [26,27]. In other words, the electrical conductivity decreases when the impact energy increases because the electrical resistance and conductivity have an inverse relationship. Moreover, impact can break partial carbon structure and then decrease the conductivity. The lower conductivity can lead to higher temperature than a sound area by eddy current in the heating phase. Consequently, the impact area will still show the higher temperature (hot spot) than sound area in the heat phase under both reflection mode and transmission mode. In addition, impact can cause delamination (disbonding between adjacent plies) when the impact energy is large enough. The temperature variation by delamination should be considered in impact analysis.

3. Experimental program

3.1. Eddy current pulsed thermography set-up

Eddy current pulsed thermography system is developed in School of Electrical and Electronic Engineering, Newcastle University, UK, as shown in Fig. 2 [11]. An Easyheat 224 from Cheltenham Induction Heater is used for coil excitation, which has a maximum excitation power of 2.4 kW, a maximum current of 400A_{rms} and an

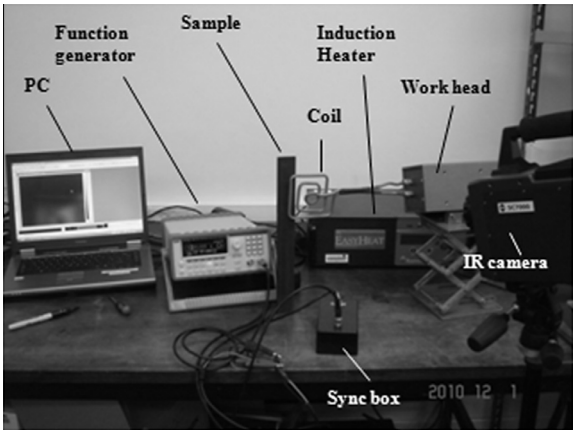

Fig. 2. Eddy current pulsed thermography system.

excitation frequency range of 150–400 kHz. The rectangular coil is constructed from 6.35 mm high-conductivity hollow copper tube and used as the eddy current stimulation. Water is pumped through the coil during operation to aid in cooling. The camera is Flir SC7500, which is a Stirling cooled camera with a 320 × 256 array of 1.5–5 μm InSb detectors. The camera has a sensitivity of <20 mK and a maximum full frame rate of 383 Hz. The resolution is 30 μm. In the experiments, the thermograms are captured using the commercial software Altair and the unit of temperature is digital level (DL). The function generator is used to control the IR camera and induction heater. PC is used to set the parameters for camera and save the detection date.

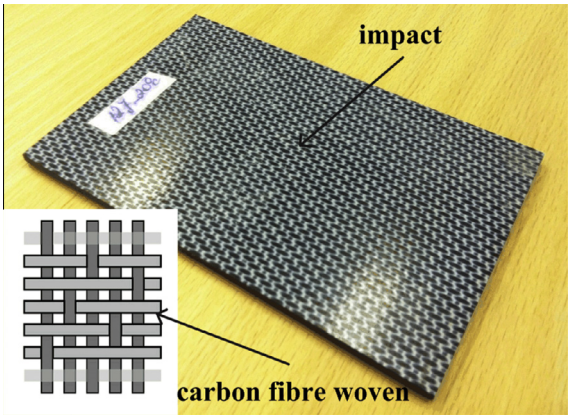

Fig. 3. Photo of CFRP impacted laminate.

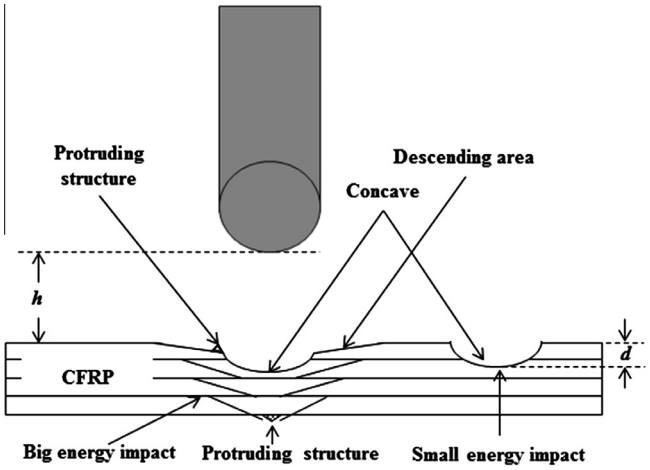

Fig. 4. General impact characteristics for CFRP structures.

3.2. Specimens

As shown in left bottom figure in Fig. 3, CFRP samples have 12 layers of 5HS carbon fiber woven with balanced woven fabric [28]. The polymer matrix is made of Polyphenylene sulphide (PPS), a thermoplastic resin system [29]. The size of the plate is 100 × 150 mm^2 and the average thickness is 3.78 ± 0.05 mm. The sample is with a 0.5 ± 0.03 volume ratio and 1460 kg/m^3 density. The plates are produced by TenCate Advanced Composites, Netherlands. As illustrated in Fig. 4, impact is fabricated in the middle of sample by free-hall of the hammer and the energy can be calculated by Eq. (1):

$$W = mgh \tag{1}$$

where m is the quality of hammer and h is the height of hammer before free-hall. In the experiments, m is 2 kg and h is various from 0.1 to 0.6 m in step of 0.1 m. Thus, the impact energy W can be calculated as 2, 4, 6, 8, 10 and 12 J in sequence. General impact characteristics for CFRP structures are illustrated in Fig. 4. The small energy impact can result in a concave on the surface of the specimen. The big energy impacts can lead to not only a concave, but also the descending area outside of concavity, some protruding structure on the edge of concavity and on the rear side of sample. Fig. 5a and b shows the front side and rear side of 12 J impacted laminate using microscope. Clearly, some protruding structures are around the concavity on the front side while the protruding structures are in the middle of impact spot on the rear side. As shown in Fig. 5c–e for rear sides of 10 J, 8 J and 6 J impacted laminates, the protruding structures are decreased as the impact energy decrease. There is no protruding structure found on the rear sides of 2 J and 4 J impacted laminates.

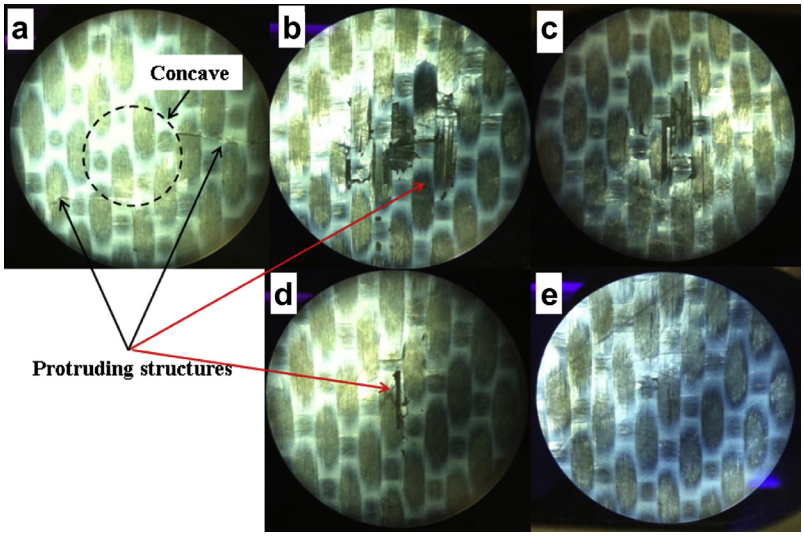

Fig. 5. (a) front side of 12 J impacted laminate; (b) rear side of 12 J impacted laminate; (c) rear side of 10 J impacted laminate; (d) rear side of 8 J impacted laminate; and (e) rear side of 6 J impacted laminate.

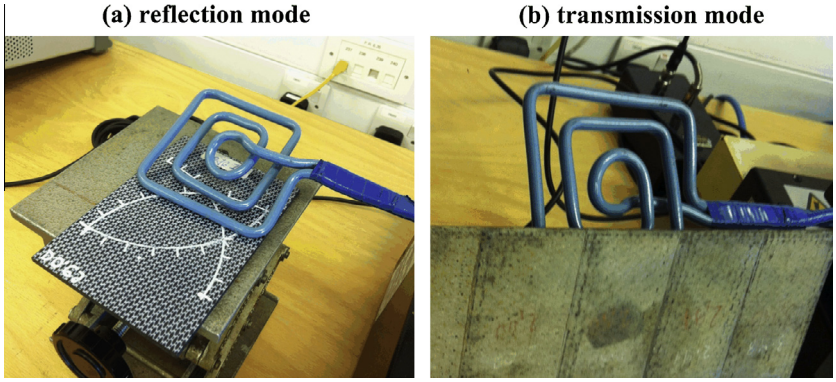

Fig. 6. Set-up under (a) reflection mode and (b) transmission mode.

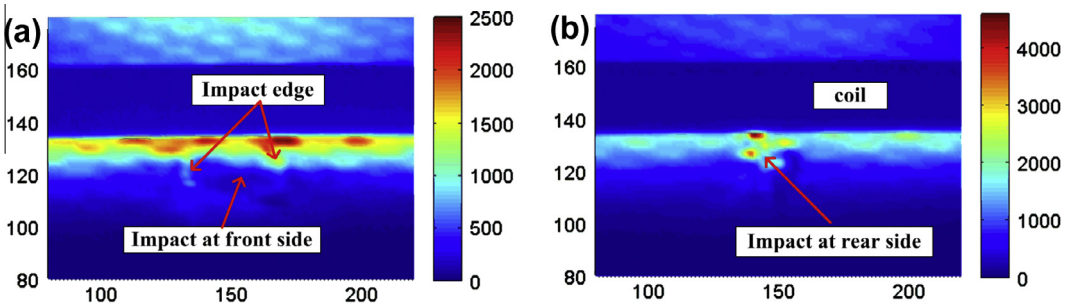

Fig. 7. Thermograms for front side and rear side of 10 J impacted laminate at 200 ms under reflection mode.

4. Results and discussion

4.1. Impact detection from thermograms

The impact laminates are tested using eddy current pulsed thermography under reflection mode shown in Fig. 6a and transmission mode shown in Fig. 6b, respectively.

The signal-to-noise ratio depends on the heating of the sample, which in turn depends on the power and the heating time. Therefore, the greater heating time can lead to the higher signal-to-noise. However, thermal diffusion process can lead to the blurring of the image over time. As the power of the generator is limited, a compromise is necessary to get enough heat into the material under test and to have a good contrast in the image. This compromise is quite easy for most materials and results in heating time of about 50–200 ms [30]. In the experiments under reflection mode, the heating time is set after optimisation and comparison as 200 ms and the cooling time is set as 300 ms. Firstly, the front side of 10 J impact sample is tested. Fig. 7 shows the thermograms for front side and rear side of 10 J impacted laminate at 200 ms. The unit for *x*-axis and *y*-axis is pixel and the unit of temperature is digital level (DL). In Fig. 7a, there is a circle shape of higher temperature around impact. However, the middle area (concavity with thinner thickness) does not show the higher temperature. In Fig. 7b, the higher temperature distribution is concentrated.

In the experiments under transmission mode, the front side and rear side of 10 J impacted laminate are tested, respectively. In order to let heat conduct from surface to rear side, the greater heating time (1 s) and cooling time (500 ms) are applied. Some points (A, B, C, D and E) are selected to observe the temperature variation. Their locations are listed in Table 1. Fig. 8 shows the thermogram of front side of 10 J impacted laminate at 50 ms under transmission mode. The carbon fiber structure (including A and C) is clear and matrix (including B and D) is low temperature. However, it is difficult to identify the impact. Fig. 9 shows the thermograms of front side and rear side of 10 J impacted laminate at 1 s under transmission mode. In Fig. 9a, points A–D show the high temperature and there is a circle shape higher temperature around impact like Fig. 7a. However, the middle area (concavity) does not show the higher temperature. The circle shape of higher temperature indicates that the lower conductivity caused by impact is focused

Table 1
The locations of points A, B, C, D and E on 10 J impacted laminate.

Point name	Location (carbon fiber or matrix)	Location (defect or good part)
A	Carbon fiber	Impact edge
B	Matrix	Impact edge
C	Carbon fiber	Defect-free
D	Matrix	Defect-free
E	Matrix	Impact middle

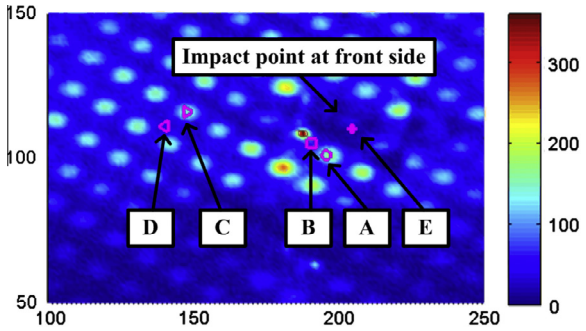

Fig. 8. Thermogram for front side of 10 J impacted laminate at 50 ms under transmission mode.

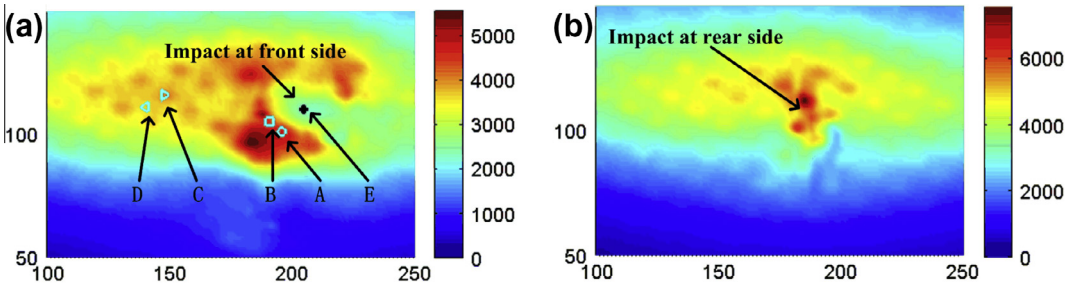

Fig. 9. Thermograms for front side and rear side of 10 J impacted laminate at 1 s under transmission mode.

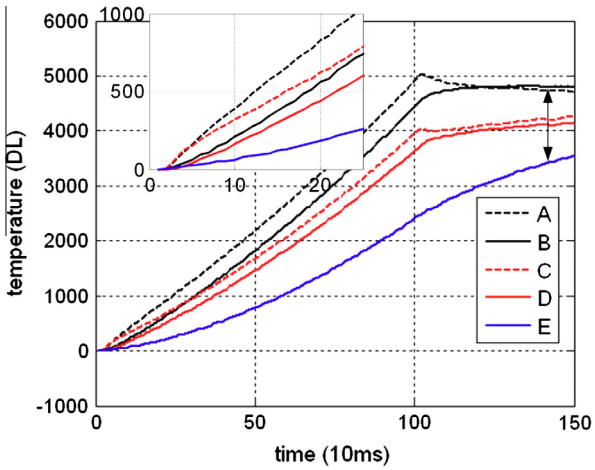

Fig. 10. Temperature responses for different points on 10 J impacted laminate under transmission mode.

on the impact edge but not in the middle on the surface. In Fig. 9b, the higher temperature by impact is like that in Fig. 7b. In this area, the partial broken structure leading to the lower conductivity is concentrated, as displayed in Fig. 5c.

4.2. Impact characterization from temperature response

Obviously, the fiber structure and polymer matrix will show the different transient temperature responses due to specific electric and thermal properties. Table 1 describes the locations of some points on front side of 10 J impacted laminate. Figs. 8 and 9a show the locations on the thermograms. Fig. 10 shows the temperature responses for points A, B, C, D and E. Point E in the middle of impact area always show the smaller temperature than good parts (C and D) and impact edge (A and B). Point A and C have similar temperature in early stage (50 ms). Points B and D also have the similar temperature in early stage (50 ms). And points A and C show the higher temperature than points B and D (250 ms), because points A and C are on the conductive carbon fiber. However, after 500 ms, points A and B show the higher temperature than points C and D until to 1 s, which illustrate the conductivity change by impact begin to affect the temperature change. In the cooling phase, points A and B still show the higher temperature than points C and D. The results illustrate that the early stage of heating phase

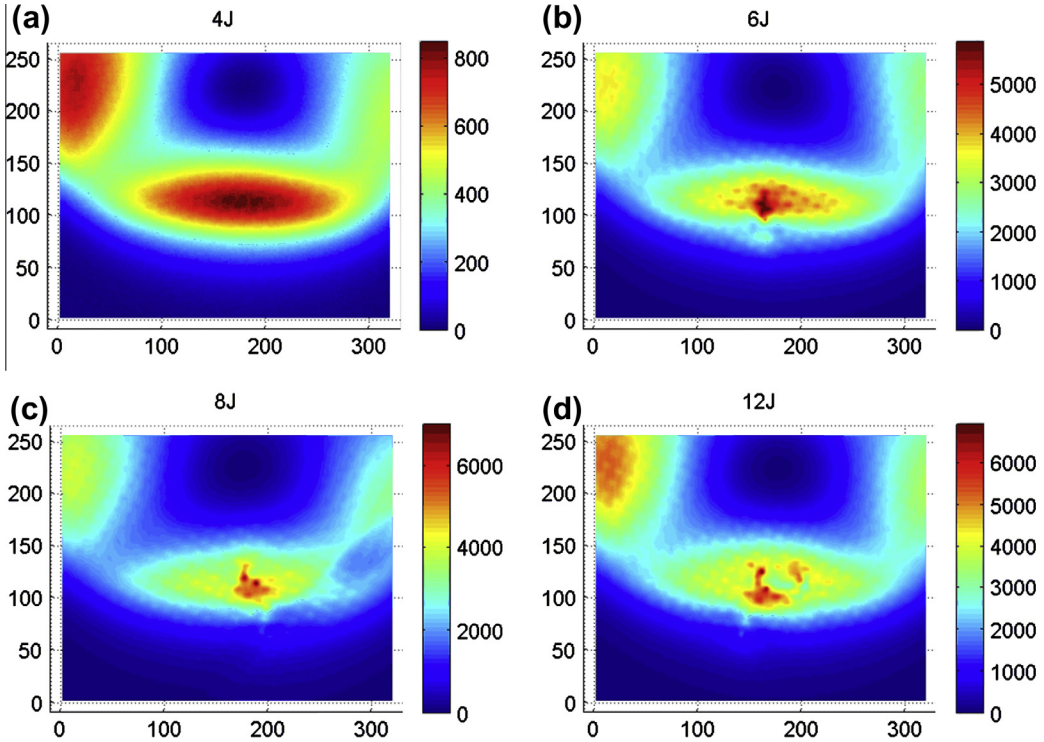

Fig. 11. Thermograms for the front sides of 4 J, 6 J, 8 J and 12 J impacted laminates.

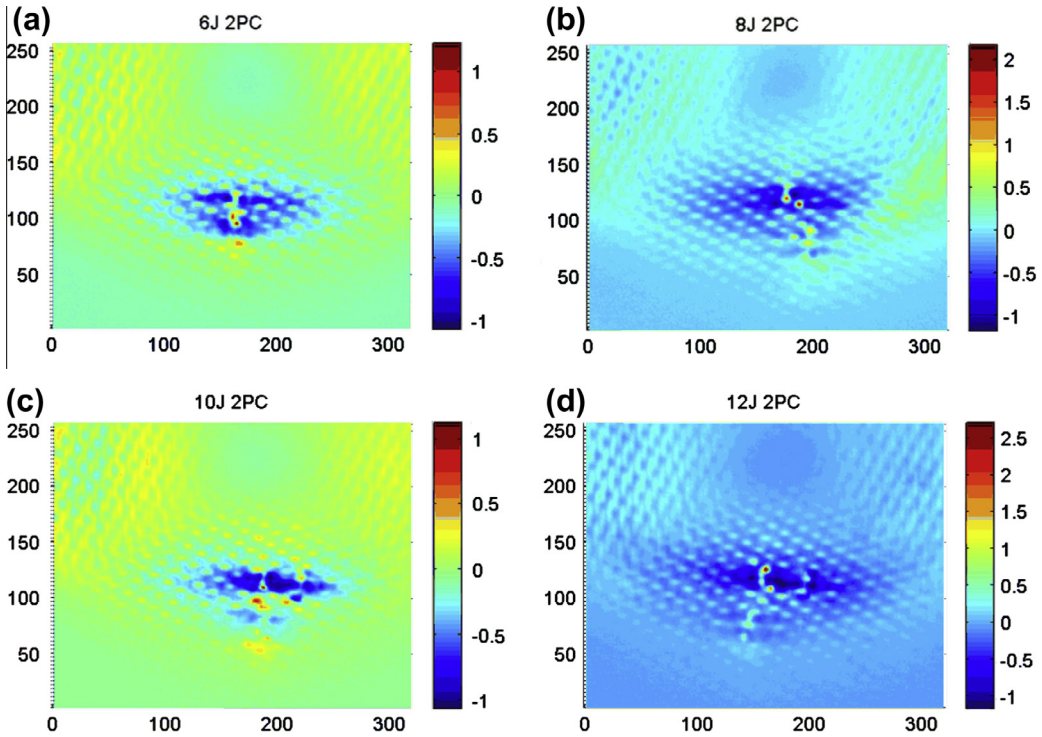

Fig. 12. Thermograms reconstructed by principal components analysis for the front sides of 4 J, 6 J, 8 J and 12 J impacted laminates.

is suitable for carbon fiber mapping and that both latter heating phase and cooling phase can be used for impact characterization.

Both results under reflection mode and transmission mode illustrate that the detection of impact is mainly based on the carbon structure broken and conductivity change but not the thickness change using eddy current pulsed thermography. The carbon structure broken and lower conductivity can lead to the remarkable difference from sound area in eddy current heat phase.

4.3. Impact energy vs. damage

The front sides of 4 J, 6 J, 8 J and 12 J impacted laminates are tested under transmission mode. Fig. 11 shows the thermograms at 1 s from raw data using Altair software and Fig. 12 shows the thermograms reconstructed by principal components analysis [31,32]. Obviously, 4 J impact cannot be observed from both raw data and reconstructed image. The hot temperature areas by 6 J and 8 J impacts are concentrated. 10 J and 12 J impacts lead to the circle shaped hot temperature distribution. The hot area (circle or point) can be used to identify the impact and predict the impacted size. However, it is difficult to extract the characteristic features to accurately quantify the impact energy from current work, which will be dug out in forthcoming work.

5. Conclusions

In this paper, an emerging NDT technique, eddy current pulsed thermography is investigated for CFRP testing and impact evaluation. The main contribution of this work includes:

(i) The detection mechanisms and qualitative conclusions are outlined and validated by experimental studies. Carbon fiber structure and impact leading to lower conductivity can be detected directly in the heating phase.

(ii) Impact shows the different hot spot shapes at the thermograms. The impact behavior for real damages are drawn. The hot area by impacts with 10 J and 12 J is like circle shape; the hot area by impact with 6 J and 8 J is concentrated; 2 J and 4 J impacts cannot be detected;

(iii) Two detection modes are compared. Reflection mode is more suitable for in situ inspection, because there is no direct access to both sides for many practical components. However, the transmission mode is more suitable for manufacturing and testing, because the coil does not affect the camera view to object under this mode.

The future work will focus on improved experimental studies for damage localisation, material differentiations (like electrical conductivity, thermal conductivity, and diffusivity) evaluation caused by impact.

Acknowledgments

The work was supported by the EPSRC grants EP/E005071, UK, National Natural Science Foundation of China Grants 61171134. The authors would like to thank Prof. Grimberg in National Institute of Research and Development for Technical Physics, Romania for providing the experimental CFRP samples. The authors are also grateful to China Scholarship Council for sponsoring Mr. Yunze He's joint PhD study to Newcastle University, UK.

References

[1] Kirkby E, de Oliveira R, Michaud V, Månson JA. Impact localisation with FBG for a self-healing carbon fibre composite structure. Compos Struct 2011;94(1):8–14.

[2] Kaczmarek H. Ultrasonic detection of the development of transverse cracking under monotonic tensile loading. Compos Sci Technol 1993;46(1):67–75.

[3] Park J-M, Kim P-G, Jang J-H, Wang Z, Kim J-W, Lee W-I, et al. Self-sensing and dispersive evaluation of single carbon fiber/carbon nanotube (CNT)-epoxy

composites using electro-micromechanical technique and nondestructive acoustic emission. Compos B Eng 2008;39(7–8):1170–82.
[4] Kordators EZ, Aggelis DG, Matikas TE. Monitoring mechanical damage in structural materials using complimentary NDE techniques based on thermography and acoustic emission. Compos B Eng 2012; 2012(43):2676–86.
[5] Frieden J, Cugnoni J, Botsis J, Gmür T. Low energy impact damage monitoring of composites using dynamic strain signals from FBG sensors – Part I: Impact detection and localization. Compos Struct 2012;94(2):438–45.
[6] Takeda S, Aoki Y, Nagao Y. Damage monitoring of CFRP stiffened panels under compressive load using FBG sensors. Compos Struct 2012;94(3):813–9.
[7] De Goeje MP, Wapenaar KED. Non-destructive inspection of carbon fibre-reinforced plastics using eddy current methods. Composites 1992;23(3):147–57.
[8] Bin Sediq AS, Qaddoumi N. Near-field microwave image formation of defective composites utilizing open-ended waveguides with arbitrary cross sections. Compos Struct 2005;71(3–4):343–8.
[9] Garnier C, Pastor M-L, Eyma F, Lorrain B. The detection of aeronautical defects in situ on composite structures using NonDestructive Testing. Compos Struct 2011;93(5):1328–36.
[10] Lyle KH, Fasanella EL. Permanent set of the space shuttle thermal protection system reinforced carbon–carbon material. Compos A Appl Sci Manuf 2009;40(6–7):702–8.
[11] Wilson J, Tian GY, Abidin IZ, Yang S, Almond D. Pulsed eddy current thermography: system development and evaluation. Insight: Non-Destructive Test Condition Monit 2010;52(2):87–90.
[12] Bohm J, Wolter KJ. Inductive excited lock-in thermography for electronic packages and modules. In: 33rd Intertional spring seminar on electronics technology. Warsaw, Poland: IEEE; 2010.
[13] He Y, Pan M, Tian GY, Chen D, Tang Y, Zhang H. Eddy current pulsed phase thermography for subsurface defect quantitatively evaluation. Appl Phys Lett 2013;103(14):144108.
[14] He Y, Tian GY, Pan M, Chen D. Eddy current pulsed phase thermography and feature extraction. Appl Phys Lett 2013;103(8):084104.
[15] He Y, Luo F, Pan M, Hu X, Liu B, Gao J. Defect edge identification with rectangular pulsed eddy current sensor based on transient response signals. NDT and E Int 2010;43(5):409–15.
[16] Zainal Abidin I, Yun Tian G, Wilson J, Yang S, Almond D. Quantitative evaluation of angular defects by pulsed eddy current thermography. NDT and E Int 2010;43(7):537–46.
[17] He Y, Pan M, Luo F. Defect characterisation based on heat diffusion using induction thermography testing. Rev Sci Instrum 2012;83(10):104702.
[18] Cheng L, Tian G. Surface crack detection for carbon fibre reinforced plastic (CFRP) materials using pulsed eddy current thermography. IEEE Sens J 2011. p. 1–1.
[19] Tashan J, Al-mahaidi R. Investigation of the parameters that influence the accuracy of bond defect detection in CFRP bonded specimens using IR thermography. Compos Struct 2012;94(2):519–31.
[20] Oswald-Tranta B, Walle G, Oswald J. A semi-analytical model for the temperature distribution of thermo inductive heating. Padova, Italy: QIRT; 2006.
[21] Wilson J, Tian GY, Abidin IZ, Yang S, Almond D. Modelling and evaluation of eddy current stimulated thermography. Nondestructive Test Eval 2009;3:1–14.
[22] Netzelmann U, Walle G. Induction thermography as a tool for reliable detection of surface defects in forged components. In: 17th World conference on nondestructive tesing, Shanghai; 2008.
[23] He Y, Pan M, Luo F, Tian G. Pulsed eddy current imaging and frequency spectrum analysis for hidden defect nondestructive testing and evaluation. NDT and E Int 2011;44:344–52.
[24] He Y, Tian G, Zhang H, Alamin M, Simm A, Jackson P. Steel corrosion characterisation using pulsed eddy current systems. IEEE Sens J 2012;12(6):2113–20.
[25] Pratap SB, Weldon WF. Eddy currents in anisotropic composites applied to pulsed machinery. IEEE Trans Magn 1996;32(2):437–44.
[26] Hou L, Hayes SA. A resistance-based damage location sensor for carbon-fibre composites. Smart Mater Struct 2002;11:966–9.
[27] Wicks SS, De Cilloria RG, Wardle VL. Tomographic electrical resistance-based damage sensing in nano-engineered composite structures. In: 51st AIAA/ASME/ASCE/AHS/ASC Structures, Structural Dynamics and Materials Conference; 2010.
[28] Akkerman R. Laminate mechanics for balanced woven fabrics. Compos Parts B Eng 2006;37:108–16.
[29] Grimberg R, Savin A, Steigmann R, Serghiac B, Bruma A. Electromagnetic non-destructive evaluation using metamaterials. Insight: Non-Destructive Test Condition Monit 2011;53(3):132–7.
[30] Vrana J, Goldammer M, Bailey K, Rothenfusser M, Arnold W. Induction and conduction thermography: optimizing the electromagnetic excitation towards application. Rev Quant Nondestructive Eval 2009;28:518–25.
[31] Pan M, He Y, Tian GY, Chen D, Luo F. Defect characterisation using pulsed eddy current thermography under transmission mode and NDT applications. NDT and E Int 2012;52:28–36.
[32] Tian G, He Y, cheng L, Jackson P. Pulsed Eddy Current thermography for corrosion characterisation. Int J Appl Electromagnet Mech 2012;39(4):269–76.